Cyclic motifs as the governing topological factor in time-delayed oscillator networks

Anders Nordenfelt, Alexandre Wagemakers, and Miguel A. F. Sanjuán
Departamento de Física, Universidad Rey Juan Carlos, Tulipán s/n, 28933 Móstoles, Madrid, Spain
(Received 18 July 2014; published 24 November 2014)

We identify the relative amount of short cyclic motifs as an important topological factor in networks of time-delayed Kuramoto oscillators. The patterns emerging from the cyclic motifs are most clearly distinguishable in the average frequency and the momentary frequency dispersion as a function of the time delay. In particular, the common distinction between bidirectional and unidirectional couplings is shown to have a decisive effect on the network dynamics. We argue that the behavior peculiar to the sparsely connected unidirectional random network can be described essentially as the lack of distinguishable patterns originating from cyclic motifs of any specific length.

DOI: 10.1103/PhysRevE.90.052920 PACS number(s): 05.45.−a, 89.75.−k

I. INTRODUCTION

The influence of various topological features on the dynamics of complex networks forms an intriguing, though also often elusive, area of investigation [1–3]. A model often studied in this context is the Kuramoto model [4] which, despite its simple and abstract form, is able to capture many aspects of seemingly more complicated systems. For example, within the area of physics, it has been applied successfully to arrays of Josephson junctions [5] and neuron networks with time-delayed interactions [6]. The time-delayed Kuramoto model has already been investigated extensively [7–11]. In particular, the topic of cyclic motifs was treated in a paper by D'Huys *et al.* [10] where implicit equations were derived for the locking frequencies of unidirectional and bidirectional cycles. In this paper, we will show how these equations provide a heuristic explanation for the difference in behavior between networks of time-delayed Kuramoto oscillators that contain different proportions of short cyclic motifs. The importance of specific network motifs in biological systems has, for a long time, been an active area of research often involving statistical techniques [12]. Our approach, on the other hand, is not statistical. Instead, we will make use of exact analytical results obtained on isolated cyclic motifs to explain the overall behavior of complex networks where these motifs form the main building block.

A fundamental question for any network is whether the connections are unidirectional or bidirectional. For example, in a social network, acquaintances are most likely to be bidirectional (mutual). On the other hand, the links between internet pages are often unidirectional. The problem dealt with in this paper was first encountered when studying precisely this distinction on a sparsely connected network of Kuramoto oscillators with unitary natural frequency and time-delayed interactions:

$$\dot{\phi}_i(t) = 1 + \frac{K}{d}\sum_{j=1}^{N} a_{ij}\sin[\phi_j(t-\tau) - \phi_i(t)]. \qquad (1)$$

Here, τ is the time delay and K is the coupling strength, for which we always chose the value $K = 0.1$ in our computer simulations. The coefficients a_{ij}, which take the value zero or one, make up the connectivity matrix. We always require that $a_{ii} = 0$. The *node degree* of oscillator i is defined as the number of incoming connections or, equivalently, the number of nonzero coefficients a_{ij} for fixed i. The normalizing factor d is always taken as the *average node degree*. A coupling between two oscillators i and j is said to be bidirectional if $a_{ij} = a_{ji} = 1$. If, on the other hand, only one of the coefficients is equal to one, then the coupling is said to be unidirectional.

The initial motivation for the problem was formulated as the difference in behavior between networks containing (almost) exclusively either one of these types of connections. However, our explanation is best understood if we consider the bidirectional coupling as a unidirectional cycle of length two. In general, a unidirectional cycle of length n is defined as an ordered set (up to rotational symmetry) of n distinct indices $(i,j,k,\ldots,x)$ such that $a_{ij} = a_{jk} = \cdots = a_{xi} = 1$.

II. THE NETWORKS

We will develop our line of argument by considering four different classes of networks, denoted by B, T, Q, and U. These classes of networks are defined by the algorithm used to construct them. First, we specify the total number of nodes N in the network and the average node degree d. Hence, from the outset, we have thereby fixed the total number of connections (number of nonzero a_{ij}) to be exactly $N \times d$. We will only consider sparsely connected networks for which $d \ll N$.

Starting from an all-zero connectivity matrix ($a_{ij} \equiv 0$), for network B, pairs of indices (i,j) were chosen successively at random and if, at each step, the coefficients a_{ij} and a_{ji} were zero, they were both set equal to one. This process was continued until the total number of connections had reached $N \times d$. For network T, the algorithm was the same except that ordered triplets (i,j,k) were chosen successively at random, and, if a_{ij}, a_{jk}, and a_{ki} were all zero, they were put equal to one, again until the total number of connections had reached $N \times d$. In this way, the networks B and T were "doped" with unidirectional cycles of length two and three, respectively. Correspondingly, for network Q, ordered quadruples were chosen in the same manner, forming unidirectional cycles of length four. The cycle length used in the construction of these networks will be referred to as the *formative cycle length*. Finally, we let U denote the well-known unidirectional random network where, simply, $N \times d$ *ordered* pairs of indices (i,j) for which $a_{ij} = 1$ were chosen randomly with no additional structure added. (We always require that $i \neq j$.) It must be

emphasized, however, that because of the random selection of nodes, all of our networks may contain cycles of any length within the limits set by the network size. Moreover, for all network classes, the node degree distribution will not be identical. The algorithms merely guarantee that networks B, T, and Q have a larger number of certain short cyclic motifs, as compared to network U.

Regarding network U, we can state the following standard analytical results: The degree distribution will be binomial and the expectation value $C(k)$ for the number of directed cycles of length k is given by

$$C(k) = \frac{p^k}{k}\binom{N}{k}. \tag{2}$$

Here, p is the probability for the existence of a connection between two randomly chosen nodes, which in our case is equal to $p = d/(N-1)$. Clearly, for network U, the number of short cyclic motifs depends strongly on both the network size N and the average degree d. If we keep d fixed, the number of short cycles relative to the network size diminishes as N increases. Our decision to limit the study to include only sparsely connected networks can now be motivated more clearly. If the connection density d were to be given a value of the same order of magnitude as the network size N, then all of the networks would become dominated by bidirectional couplings and the distinction between the networks would be of no use for our analysis.

In Sec. IV, we will have reason also to consider a slightly modified family of networks constructed with the extra condition that all node degrees be the same. These modified networks, denoted by $B*$, $T*$, $Q*$, and $U*$, were constructed with the same algorithms already described for networks B, T, Q, and U, with the only difference being that at each step we also made sure that no node degree surpassed the value d. With the exception of network $U*$, one is likely to face problems carrying this through consistently at the very last step since the remaining nodes might not be able to form an additional cycle (they may have already formed a cycle). When encountered, this problem was solved by simply choosing some random unidirectional couplings for the remaining nodes, which had no visible effect on the overall result.

For our computer simulations, we chose the network parameters $N = 150$ and $d = 4$. The average number of cycles of length two, three, and four of each class of networks is presented in Table I. For network B and $B*$, the number of 3 and 4 cycles are put in parentheses since, although counted correctly according to our definition, they all form part of the bidirectional cycles which behave differently as compared to pure unidirectional cycles; see Ref. [10].

TABLE I. Average number of unidirectional cycles of length two, three, and four for all network classes considered. For each class, averages were taken over a total of 32 network realizations where the total number of nodes was set to $N = 150$ and the average node degree to $d = 4$.

	Cycle length		
Networks	2	3	4
B	300	(20)	(65)
T	8	220	128
Q	8	37	276
U	8	21	63
$B*$	300	(8)	(4)
$T*$	6	206	13
$Q*$	6	19	50
$U*$	8	21	16

III. AVERAGE FREQUENCY

For a given time interval T, we define the average frequency Ω_i of each individual oscillator as follows:

$$\Omega_i \equiv \frac{1}{T}\int_0^T \dot{\phi}_i(t)dt, \tag{3}$$

from which we calculate the *average network frequency* as

$$\Omega = \frac{1}{N}\sum_i \Omega_i. \tag{4}$$

In order to interpret the results of our computer simulations, we recollect the analytical formulas presented in the paper by D'Huys *et al.* [10] for the locking frequencies ω of an isolated unidirectional cycle of length n,

$$\omega = 1 + K\sin(\Delta\phi - \omega\tau), \tag{5}$$

where the phase difference $\Delta\phi$ between each neighboring oscillator is given by

$$\Delta\phi = \frac{2j\pi}{n}, \quad 0 \leqslant j < n. \tag{6}$$

Moreover, the locking frequency ω is stable if

$$K\cos(\Delta\phi - \omega\tau) > 0. \tag{7}$$

In Fig. 1, we have plotted the average network frequency Ω as a function of time delay, calculated from computer simulations on each class of networks separately. These results do not depend on the initial conditions. In the same graph, we have superimposed (marked with red curves) the stable locking frequencies, given by Eq. (5), for the cycle length corresponding to that with which the network was doped. In the case of network U, we have included only the in-phase stable locking frequencies common to all cycle lengths. These correspond to $j = 0$ in formula (6). We observe that at every time delay, the average frequency curve tends to be attracted to the stable locking frequency that is closest to the natural unit frequency. When monitoring the overall phase coherence in the network, it is also clear that when the frequency is attracted to the stable in-phase locking frequencies ($j = 0$), the network stays in a completely or partially phase-synchronized state, whereas when the frequency starts to get attracted to the out-of-phase stable locking frequencies ($j \neq 0$), the network enters into a state almost completely out of phase. For further discussion on the phase synchronization order parameter, see Refs. [6,11].

Focusing on the middle region, we have placed the graphs in an order so as to visually convey the gradual change from the pronounced oscillation in average frequency in the case of

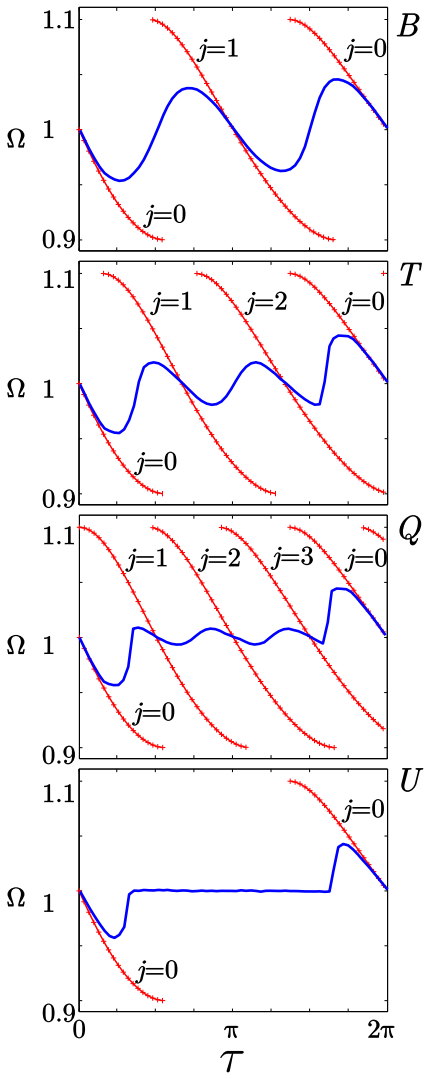

FIG. 1. (Color online) Average network frequency Ω (blue lines) as a function of time delay, calculated from computer simulations on the network classes B on top, followed by T, Q, and finally U at the bottom. The red curves mark the stable locking frequencies, given by Eq. (5), for the cycle length corresponding to that with which the network was doped. For each network class, averages were taken from a total of 32 network realizations with $N = 150$ and $d = 4$.

network B to the almost flat curve in the case of network U. Based on this observation, it might be tempting to interpret the results obtained on network U as the *limiting case* as the formative cycle length increases. However, there are some cautionary remarks to be made about this interpretation. As we see it, there is nothing in the outcome that prevents us from instead viewing network U as a primary *neutral state* that does not display any characteristic cyclic patterns unless doped with the corresponding cyclic motif. With the latter interpretation, the explanation for the flattening of the frequency curve as the formative cycle length increases would be somewhat different. Essentially, for a fixed network size, it is harder to efficiently dope a network with a longer cyclic motif than a shorter one. We observe, for example, that through the algorithms we have used, it is possible for a longer cycle to be intercepted by a shorter cycle in the sense that there may be shortcuts. Moreover, as we increase the formative cycle length, the relative number of those cycles as compared to those of the same length occurring naturally in network U [given by Eq. (2)] will diminish. Hence, the other perspective would be that the above-mentioned circumstances, rather than the cycle length itself, could to a large part explain the gradual flattening of the frequency curve. We leave it as an open question which of these perspectives is the most accurate, but, in any case, we think that an appropriate way to characterize the result obtained on network U is to view it as the lack of distinguishable patterns originating from any specific cycle length.

IV. FREQUENCY DISPERSION

In a previous paper [11], the sustained frequency dispersion $\sigma^2 \equiv \langle(\Omega_i - \Omega)^2\rangle$ was studied on networks of time-delayed Kuramoto oscillators with identical natural frequencies and homogeneous time delay. One of the conclusions of this study was that a nonidentical node degree distribution (or, alternatively, nonidentical coupling strength) is a necessary condition for a nonvanishing σ^2. When simulations are performed over sufficiently long time intervals T, this conclusion still holds. However, if we look instead at the average *momentary* frequency dispersion,

$$s^2 \equiv \frac{1}{NT}\int_0^T \sum_i [\dot{\phi}_i(t) - \Omega(t)]^2 dt, \tag{8}$$

where $\Omega(t) = \sum_i \dot{\phi}(t)/N$, there will be clear patterns emerging instead from the cyclic motifs. Clearly, a nonzero σ^2 necessarily implies a nonzero s^2, but the converse is not true.

In Fig. 2, we have plotted the average momentary frequency dispersion s^2 against the time delay, calculated from computer simulations on each class of networks separately. As discussed before, part of this momentary frequency dispersion must result from the nonidentical node degree distribution present in the networks B, T, Q, and U. However, by repeating the simulations on the family of networks with identical node degree distribution [13], $B*$, $T*$, $Q*$, and $U*$, we could distinguish the remaining parts (marked with gray color) that are instead directly related to the cyclic motifs. For networks B, T, and Q, these areas show up as bumps with centers situated at the time delays where the respective stable locking frequencies, given by Eq. (5), have equal distance to the natural unit frequency and, as it happens, when the average frequency Ω crosses the unit frequency with upward slope. For network U, on the other hand, this area shows up as a continuous interval in the middle part of the graph. Also here, we can see the gradual change in appearance of the graphs as we move from network B to network U. All of the graphs contain some asymmetries which seem to persist even when averages are taken over many network realizations. Here, we are not in a position to explain these asymmetries in detail, we merely point out that since the frequency ω occurs on the right-hand side of Eq. (5), there is not a perfect mirror symmetry in the transformation $\Delta\phi \to 2\pi - \Delta\phi$ and $\tau \to 2\pi - \tau$.

In order to further clarify the difference between σ^2 and s^2, in Fig. 3 we show the sustained frequency dispersion $\sigma^2 \equiv \langle(\Omega_i - \Omega)^2\rangle$ (solid blue curves) superimposed, for

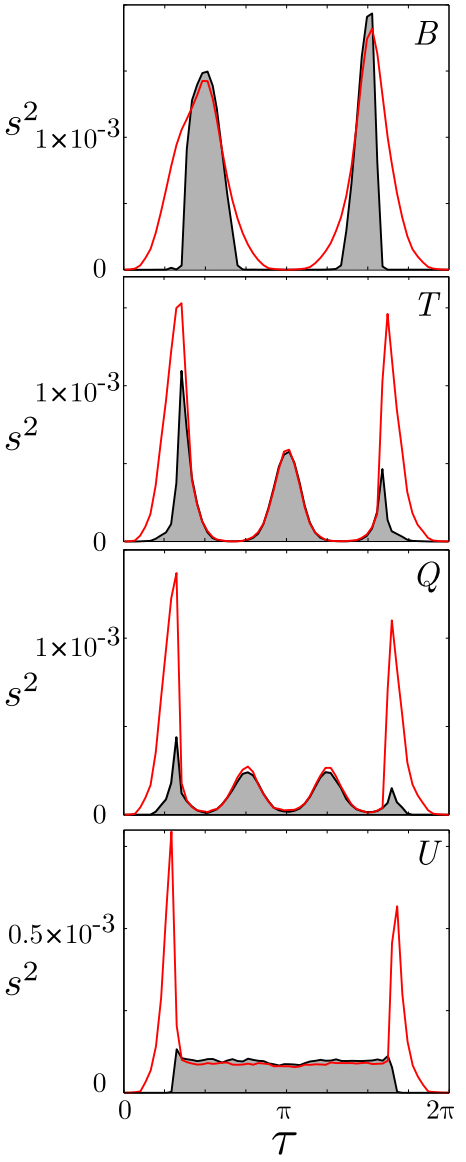

FIG. 2. (Color online) Average momentary frequency dispersion s^2 (red curves) as a function of time delay, calculated from computer simulations on the network classes B on top, followed by T, Q, and finally U at the bottom. The momentary frequency dispersion is caused in part by the nonidentical node degree distribution and in part by the cyclic motifs. The gray areas mark the dispersion that is directly related to the cyclic motifs and were found as the remaining part when the simulations were repeated on the family of networks $B*$, $T*$, $Q*$, and $U*$ constructed with the extra condition that all node degrees be the same. For each network class, averages were taken from a total of 32 network realizations with $N = 150$ and $d = 4$.

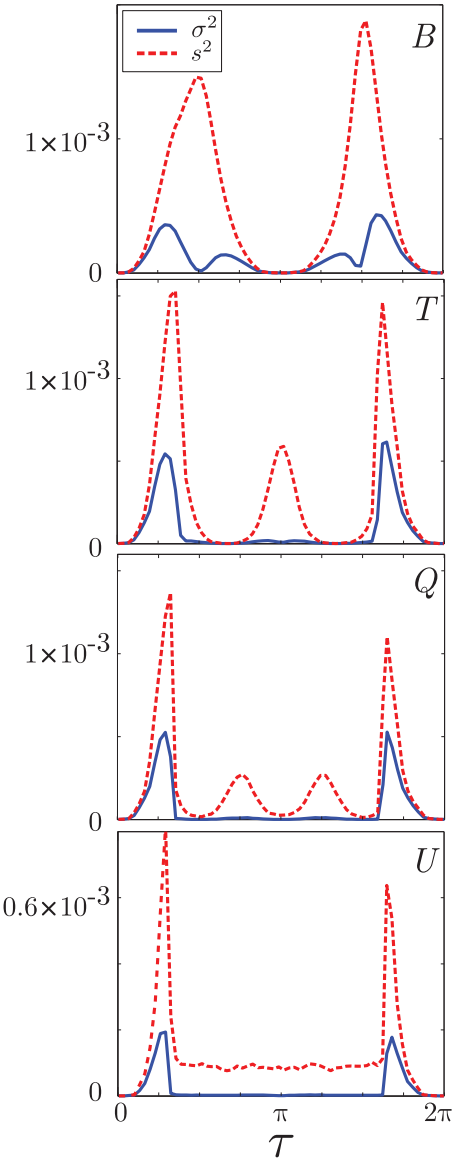

FIG. 3. (Color online) Sustained frequency dispersion σ^2 (solid blue curves) and average momentary frequency dispersion s^2 (dashed red curves) as a function of time delay, calculated from computer simulations on the network classes B on top, followed by T, Q, and finally U at the bottom. For each network class, averages were taken from a total of 32 network realizations with $N = 150$ and $d = 4$.

comparison, with the momentary frequency dispersion $s^2 \equiv \frac{1}{NT}\int_0^T \sum_i [\dot{\phi}_i(t) - \Omega(t)]^2 dt$ (dashed red curves). As we can see, in the middle region between the extremal bumps, σ^2 vanishes almost completely except for network B which, for the chosen parameters, is the only network that manages to push the average frequency sufficiently far away from the unit frequency so that, again, a noticeable sustained frequency dispersion σ^2 shows up. For further discussion on σ^2, see Ref. [11].

V. CONCLUDING REMARKS

To conclude, we have shown that one of the most important topological factors in networks of time-delayed Kuramoto oscillators is the relative amount of short cyclic motifs. Returning to our initial motivation for the study, our analysis has shown that the bidirectional random network B and the unidirectional random network U could be seen as opposite ends of a spectrum of different classes of networks. In the case of network B, the dynamics is strongly influenced by one short cyclic motif, whereas for network U, no clear pattern can be found from any specific cyclic motif. We note, in particular,

that the only time-delay region where the average frequency of U deviates from the unit frequency is where there exist stable locking frequencies common to unidirectional cycles of all lengths.

ACKNOWLEDGMENT

Financial support from the Spanish Ministry of Science and Innovation under Project No. FIS2013-40653-P is acknowledged.

[1] F. M. Atay, J. Jost, and A. Wende, Phys. Rev. Lett. **92**, 144101 (2004).
[2] A. E. Motter, C. Zhou, and J. Kurths, Phys. Rev. E **71**, 016116 (2005).
[3] A. Arenas, A. DiazGuilera, and C. J. Pérez-Vicente, Phys. Rev. Lett. **96**, 114102 (2006).
[4] Y. Kuramoto, *Chemical Oscillations, Waves, and Turbulence* (Springer, Berlin, 1984).
[5] K. Wiesenfeld, P. Colet, and S. H. Strogatz, Phys. Rev. Lett. **76**, 404 (1996).
[6] A. Nordenfelt, J. Used, and M. A. F. Sanjuán, Phys. Rev. E **87**, 052903 (2013).
[7] H. G. Schuster and P. Wagner, Prog. Theor. Phys. **81**, 939 (1989).
[8] M. K. S. Yeung and S. H. Strogatz, Phys. Rev. Lett. **82**, 648 (1999).
[9] M. G. Earl and S. H. Strogatz, Phys. Rev. E **67**, 036204 (2003).
[10] O. D'Huys, R. Vicente, T. Erneux, J. Danckaert, and I. Fischer, Chaos **18**, 037116 (2008).
[11] A. Nordenfelt, A. Wagemakers, and M. A. F. Sanjuán, Phys. Rev. E **89**, 032905 (2014).
[12] *Analysis of Biological Networks*, edited by B. H. Junker and F. Schreiber (Wiley, New York, 2008).
[13] It is important to note that networks with identical node degrees have a stable in-phase synchronized state [9] that persists for much longer time delays than is the case for networks with, for example, a binomial node degree distribution. Hence, the initial conditions are very important. Consistently, on networks $B*$, $T*$, $Q*$, and $U*$, we used the initial conditions $\phi_j(0) = 2\pi j/N$.